PRESTACK MIGRATION BASED ON ASYMMETRIC WAVE-EQUATION EXTRAPOLATION

CHIYUAN REN[1] and XIN TIAN[2]

[1] *College of Science, Southwest Petroleum University, Chengdu 610500, P.R. China.*
renchiyuan@163.com
[2] *Applied Technology College, Southwest Petroleum University, Chengdu 610500, P.R. China.*

(Received May 25, 2015; revised version accepted April 7, 2016)

ABSTRACT

Ren, C. and Tian, X., 2016. Prestack migration based on asymmetric wave-equation extrapolation. *Journal of Seismic Exploration*, 25: 375-397.

Prestack wave-equation migration has been popular in recent years. One-way wave equation migration and two-way wave-equation migration are the two choices for applying the wave-equation migration. They have different advantages and disadvantages. In this investigation, a combined version of these methods is developed, called asymmetric wave-equation migration. In this migration scheme, the source wave-field is extrapolated using the one-way wave-equation or two-way wave-equation, but the receiver wave-field is extrapolated based on the wave-equation being different from the former. By analyzing theoretically, the asymmetric wave-equation migration scheme can greatly reduce computation time compared with two-way wave-equation migration. Meanwhile, detailed comparisons between different migration schemes have been performed. The results show that the proposed migration scheme can work better than the two-way wave-equation migration, with less computation time and noise; thus, it is a new choice when we select migration schemes.

KEY WORDS: wave-equation migration, one-way wave-equation, two-way wave-equation, computation complexity, image quality.

INTRODUCTION

Prestack migration based on a wave equation has gained popularity recently both in academic research and engineering applications (Claerbout, 1971, 1985; Liu et al., 2007, 2008; Zhang et al., 2007). The migration method can provide a more accurate structural image of the subsurface, compared with time migration. Prestack migrations based on a wave-equation include two

0963-0651/16/$5.00

principle steps: 1) extrapolate wave-fields. The source wave-field is extrapolated from shots forward in time, while the receiver wave-field is extrapolated from receivers backward in time; 2) image by imaging condition. After wavefield extrapolation, an imaging condition is applied to the two wave-fields to form a depth image. Extrapolating wavefields using the wave-equation is the key process in the migration method. Two different strategies are employed to solve the wave equation (Mulder and Plessix, 2003). The first is to solve the full-wave equation directly. The migration scheme based on this strategy is referred to as two-way wave-equation migration. The other option is to decompose the wave-equation into an upgoing wave-equation and downgoing wave-equation (Wu, 1994; Collino and Joly, 1995; Biondo and Palacharla, 1996). The migration scheme based on this strategy is called one-way wave-equation migration.

Two-way wave-equation migration is often also called reverse time migration (RTM) and can be implemented in the time domain or in the frequency domain (McMechan, 1983; Whitmore, 1983; Baysal et al., 1983, 1984). The computation efficiency in the frequency domain is higher than that in the time domain (Mulder and Plessix, 2004). Two-way wave-equation migration can simulate wave propagation without any approximation in complex media. Therefore, the migration scheme can govern all the energy in wave-fields can image layers accurately without the limitation of dip. However, two-way wave equation migration has some shortcomings. First, it is not computationally friendly. For three dimensions, it is usually unaffordable in practice. Second, low-wavenumber artifacts, especially in shallow layers, could cover the real image and count against seismic interpretation. An additional work is usually needed to filter the image produced by two-way wave-equation migration. Third, numerical dispersion and numerical stability are problems that need to be treated carefully (Xie et al., 2014; Feng et al., 2015). To overcome these problems, more time is required in the migration scheme.

By approximations and mathematical transforms, the two-way wave-equation can be factored into two one-way wave-equations, which describe the upgoing wave and the downgoing wave, respectively. The one-way wave-equation is expressed by a pseudo-difference operator, which cannot be solved directly. Thus, many researchers have developed different approaches to simplify the one-way wave-equation, such as the 15° wave-equation (Claerbout, 1971), 45° wave-equation (Stolt, 1978), phase-shift (Gazdag, 1978), phase shift plus interpolation (Gazdag and Sguazzero, 1984), split step Fourier (Stoffa et al., 1990), Fourier finite difference (Ristow and Ruhl, 1994), generalized pseudo screen (Jerome et al., 2001; Huang and Wu, 1996), etc. The one-way wave-equation can govern the principle energy in a wave-field, and the image produced is superior to that produced via ray-based migration. These methods are usually implemented in the frequency-wavenumber domain or frequency-space domain and extrapolate wavefields in the depth direction. Thus, compared

to two-way wave-equation migration, one-way wave-equation migration can greatly reduce computation time, especially in a 3D application. However, the one-way wave-equation is just an approximation of the two-way wave-equation; thus, it is difficult to accurately simulate wave propagation in complex media, especially with a strong lateral velocity gradient. Meanwhile, the one-way wave equation cannot govern multiples. Thus, migration based on it is under the limitation of dips, making it hard to image the steep flanks (Albertin et al., 2002). Therefore, one-way wave-equation migration cannot image layers as well as two-way wave-equation migration.

Due to their different advantages and disadvantages, the choice between one-way wave-equation migration and two-way wave-equation migration is usually hard in practice. Mulder and Plessix (2004) performed a detailed comparison between them and made some meaningful conclusions. They stated that the two migration methods are better than the other in some aspects but worse than the other in other aspects simultaneously. Thus, they made an unsatisfying suggestion: if one has sufficient computation resources, he should use the two-way wave-equation migration; if not, choose the other. Bednar et al. (2003) tried to make a final judgement and proposed a direct question regarding whether the two-way wave-equation is overkill or necessary. However, they ultimate reached a similar conclusion to that of Mulder and Plessix (2004). Thus, making a decision regarding using one-way wave-equation migration or two-way wave-equation migration is difficult in many situations due to their respective characteristics. A compromise is to use a different extrapolation approach in different districts. One-way propagator is applied in less complex districts, while the full-way propagator is applied in extremely complicated districts (Luo and Jin, 2008).

In this investigation, we develop another way to implement one-way wave-equation migration and RTM. The approach provides a new choice when we select migration schemes. The key idea is to extrapolate source and receiver wave-fields in asymmetric wave-equations: we extrapolate the source wave-field using the two-way wave-equation and extrapolate the receiver wave-field by using the one-way wave-equation, or vice-versa. Numerical simulation shows that the migration approach is of higher computational efficiency and has less artifacts than two-way wave-equation migration and is able to image the layers with steep dips. This work is organized as follows. The first section presents the definition and algorithm of prestack two-way and one-way wave-equation migrations and explains why we employ asymmetric extrapolation in migration. Then, the proposed migration scheme is described in detail and its advantages are analyzed in the next section. The third section employs two synthetic datasets to verify the performance of the proposed migration numerically. The results show that it can image without the limitation of dips and works better than the two-way wave-equation migration, with less computation time and noise. Finally, some conclusions are drawn.

THEORY

Two-way wave-equation

In this investigation, we only consider the P-wave. The governing equation can be expressed as the following expression in the 2D time-space domain.

$$\partial^2 P(X,t)/\partial t^2 = c^2 \nabla^2 P(X,t) \quad , \tag{1}$$

where P is the wave-field pressure at a spatial location X and time t, c is the media acoustic velocity, and ∇^2 is the Laplacian operator.

By using the 2-order center difference scheme, the time derivative is derived as

$$\partial^2 P^n_{i,j}/\partial t^2 = (1/\Delta t^2)[P^{n+1}_{i,j} + P^{n-1}_{i,j} - 2P^n_{i,j}] \quad . \tag{2}$$

At the same time, the spatial derivatives could be derived using the 2L-order center difference scheme:

$$\begin{aligned} \partial^2 P^n_{i,j}/\partial x^2 &= (1/\Delta x^2) \sum_{l=1}^{L} a_l [P^n_{i+l,j} + P^n_{i-l,j} - 2P^n_{i,j}] \\ \partial^2 P^n_{i,j}/\partial z^2 &= (1/\Delta z^2) \sum_{l=1}^{L} a_l [P^n_{i,j+l} + P^n_{i,j-l} - 2P^n_{i,j}] \end{aligned} \tag{3}$$

where a_l are the parameters of the high-order finite different scheme (Dablain, 1986). Thus, based on the two-way wave equation, the extrapolate scheme of the wave field can be expressed as

$$\begin{aligned} P^{n+1}_{i,j} = 2P^n_{i,j} + P^{n-1}_{i,j} &+ (c^2\Delta t^2/\Delta x^2) \sum_{l=1}^{L} a_l [P^n_{i+l,j} + P^n_{i-l,j} - 2P^n_{i,j}] \\ &+ (c^2\Delta t^2/\Delta z^2) \sum_{l=1}^{L} a_l [P^n_{i,j+l} + P^n_{i,j-l} - 2P^n_{i,j}] \end{aligned} \tag{4}$$

where Δx, Δz and Δt denote the step length of the variable x, z and t, respectively. Employing the state transfer matrix, the corresponding stability condition could be derived as

$$\Delta t \leq 2\Delta s/\sqrt{2}\sqrt{\{-a_0 + 2\sum_{l=1}^{L} a_l(-1)^{l+1}\}} \quad ,$$

$$\Delta s = \min(\Delta x,\Delta z), a_0 = -2\sum_{l=1}^{L} a_l \quad , \tag{5}$$

where v_{max} is the maximum of the velocity model.

One-way wave-equation

Eq. (1) can be transformed to the frequency-space domain, expressed as

$$\tilde{P}(X,\omega) = -(c^2/\omega^2)\nabla^2\tilde{P}(X,\omega) \quad , \tag{6}$$

where $\tilde{P}$ is the Fourier transform of P, i.e., $\tilde{P} = \int_{+\infty}^{-\infty} P\cdot e^{-2\pi i\omega t}dt$.

The one-way wave-equation requires less computational cost, particularly in three dimensions. It can be formulated using the square-root operator in two dimensions as

$$\partial\tilde{P}^{\pm}/\partial z = \mp i\sqrt{\{(\omega^2/c^2) + (\partial^2/\partial x^2)\}}\ \tilde{P}^{\pm} \quad , \tag{7}$$

where $\tilde{P}^{\pm}$ is the upgoing and downgoing wave-field in the frequency-space domain. Eq. (7) could be further transformed to the frequency-wavenumber domain via the Fourier transform of x. For an upgoing wave, it can be expressed as

$$\partial\tilde{P}^{+}(k_x,z,\omega)/\partial z = -(i\omega/c)\sqrt{\{1 - (c^2/\omega^2)k_x^2\}}\ \tilde{P}^{+}(k_x,z,\omega) \quad , \tag{8}$$

where $\tilde{P}^{+}$ is the Fourier transform of $\tilde{P}^{+}$. Based on the above equation, the wavefield can be extrapolated in depth as

$$\tilde{P}^{+}(k_x,z+\Delta z,\omega) = \tilde{P}^{+}(k_x,z,\omega)\exp[-(i\omega/c)\sqrt{\{1 - (c^2/\omega^2)k_x^2\}}\cdot\Delta z] \quad , \tag{9}$$

where Δz is the depth step and k_x is the wave number of the x-direction. Let $Y = \sqrt{\{1 - (c^2k_x^2/\omega^2)\}}$; then, Y is the phase shift operator. Unfortunately, due to the square root operator incorporated into it, the one-way wave-equation cannot be solved directly. Necessary approximations must be performed to simplify the above equation. Researchers have developed many approaches for this. These methods can be classified into two families. One is to approximate the square-root operator by using the Pade approximation, and several schemes have

been proposed (Claerbout, 1971; Wu, 1994; Collino and Joly, 1995; Biondi and Palacharla, 1996; Risow and Ruhl, 1994). The other is to transform the equation into the frequency-wavenumber domain, then to extrapolate the wave-field via phase-shift (Gazdag, 1978). However, this approach is only fit for the simulation of wave propagation in homogeneous media; thus, several advanced schemes based on it have been developed to improve its performance in complex media, such as phase-shift-plus-interpolate (Gazdag and Sguazzero, 1984), Fourier-finite-difference (Ristow and Ruhl, 1994), and split-step-Fourier (Stoffa et al., 1990).

In this investigation, a splitting method (Collino and Joly, 1995) is employed to implement the one-way wave equation extrapolation. It evaluates the square root with three terms of Pade approximation, providing good phase accuracy up to approximately 70°. However, it cannot model amplitudes correctly (Zhang et al., 2007).

Imaging condition of wave-equation migration

After the source wave-field and receiver wave-field are extrapolated based on eqs. (1) or (6), an imaging condition is conducted on the two wave-fields to form the image of layers. Many imaging conditions have been developed (Chattopadhyay and McMechan, 2008; Costa et al., 2009; Guitton et al., 2007; Sava and Fomel, 2006; Yoon and Marfurt, 2006; Ren et. al. 2015), but the most popular imaging condition is the cross-correlation imaging condition developed by Claerbout (1971) due to its simplicity and stability; it can be formulated in the time domain and frequency domain as

$$\begin{aligned} I(X) &= \sum_{\text{shots}} \sum_{t} P_S(X,t)P_R(X,t), \ \text{time}-\text{domain} \\ I(X) &= \sum_{\text{shots}} \sum_{\omega} \tilde{P}_S(X,\omega)\tilde{P}_R^*(X,\omega), \ \text{frequency}-\text{domain} \end{aligned} \tag{10}$$

where I(X) is the depth image at point X, P_S and P_R are the forward-propagating source wave-field and backward-propagating receiver wave-field, respectively, and $\tilde{P}_S$ and $\tilde{P}_R$ are the Fourier transforms of P_S and P_R for time t, respectively.

Prestack migration based on the asymmetric wave-equation

One-way wave-equation migration and two-way wave-equation migration are similar to each other but employ different wave-equations to extrapolate wave-fields. In two-way wave-equation migration, the source and receiver

wave-fields are extrapolated by using the two-way wave-equation, which can describe wave-fields accurately but is costly. However, in one-way wave-equation migration, the source and receiver wave-fields are both extrapolated by using the one-way wave-equation, which is cheap but only approximately simulates the wave-field. In other words, the governing equation of the source wave-fields is the same as the governing equation of the receiver wave-fields but uses different boundary conditions and extrapolating directions.

To integrate the advantages of one-way wave-equation migration and two-way wave-equation migration, we develop a novel migration based on the asymmetric idea. In the proposed migration scheme, the source wave-field is extrapolated using the two-way wave-equation or one-way wave-equation, while the receiver wavefield is extrapolated by using the wave-equation not used to extrapolate the source wave-field. Hence, the asymmetric migration has two forms. If the source wave-field is extrapolated by using the two-way wave equation and the receiver wave-field is extrapolated by using the one-way wave-equation in migration, we call it two-one-way wave-equation migration. The other asymmetric wave-equation migration is called one-two-way wave equation migration, where the source wavefield is extrapolated using the one-way wave-equation, while the receiver wavefield is extrapolated using the two-way wave-equation. In asymmetric wave-field migration, the two-way wave-equation is replaced with the one-way wave-equation on one side to greatly reduce the need for computation resources, particularly in three dimensions. Moreover, the proposed migration can also image via multipath as in two-way wave-equation migration.

COMPLEXITY ESTIMATES

We perform the complexity estimate following the conclusion drawn by Mulder and Plessix (2003, 2004); thus, it is partly repeated from Marfurt and Shin (1989) and Mulder and Plessix (2004). Let n be the number of grid points of every space coordinate; then, there are $O(n^2)$ or $O(n^3)$ points for a 2D grid or 3D grid, respectively. The number of frequencies is n_w, and the number of time steps is n_t. Thus, for two-way wave equation extrapolation in the time-domain, $O(n_t n^2)$ or $O(n_t n^3)$ operations are required for 2D or 3D, respectively. Otherwise, for one-way wave equation extrapolation, $O(n_w n^2)$ or $O(n_w n^3)$ operations are required for 2D or 3D, respectively. Due to the stability condition, the time step is constrained by the grid spacing; thus, n_t is proportional to n. However, n_w can be set relatively small compared to n_t; thus, it is $O(1)$. Therefore, whether for the 2D or 3D model, the complexity of one-way wave equation extrapolation is one order lower than that of two-way wave equation extrapolation. In wave equation migration, most computational time is spent on extrapolating the source wavefield and receiver wavefield. Because the complexity of two-way wave-equation extrapolation is one order

higher than that of the one-way wave equation, the time required for one-way wave-equation extrapolation could be ignored compared with the time required for two-way wave-equation extrapolation. Therefore, because the proposed asymmetric wave-equation migration only employs the two-way wave equation in forward extrapolation or backward extrapolation, computation time will be reduced by approximately half compared with two-way wave-equation migration. This is very attractive in practice.

IMAGING ABILITY EVALUATION

Fig. 1 shows the image principle of wave-equation migrations. In the figures, only one shot and one receiver are set on the surface and wave-fields are simulated coming from them, either forward or backward in time, respectively. An image point is set on a subsurface, and rays along different paths from shots and receivers can image it. The rays marked as 1 and 3 are the first waves in the source wave-field and receiver wave-field, respectively. The rays marked as 2, 4, 5 and 6 are multipath waves in the two wave-fields.

One-way wave-equation migration, as depicted in Fig. 1(a), only uses the first waves in the source and receiver wave-fields to image, which can allow for governing the main energy in the wave-fields and produces less low-wavenumber artifacts. However, two-way wave-equation migration, depicted in Fig. 1(b), can employ all waves in the wave-fields to produce images; thus, it images layers better. Unfortunately, it will produce some low-wavenumber artifacts along the path of rays at the same time, which contaminates the images, especially in the shallow layer. Many researchers have performed much work to overcome this problem. Liu et al. (2007, 2011) only used the waves propagating in opposite directions to image by decomposing the wave-fields into downgoing and upgoing wavefields. This idea was also exploited by Fei et al. (2010) and Diaz and Sava (2012) to attenuate the noise induced by the back-scattering energy. As for the proposed asymmetric wave-equation migration scheme, depicted in Fig. 1(c-d), it only uses the main energy governed by the one-way wave-equation on the one side and retains the ability of imaging by allowing multiple waves to govern via the two-way wave-equation on the another side. This indicates that the asymmetric wave-equation migration is able to image via multiples, as in two-way wave equation migration, while producing fewer low-wavenumber artifacts, which is beneficial to the further work after imaging. However, its performance for real data sets needs to be verified.

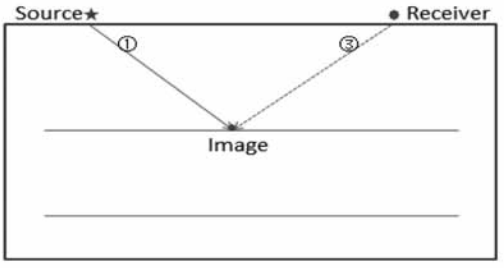

(a)

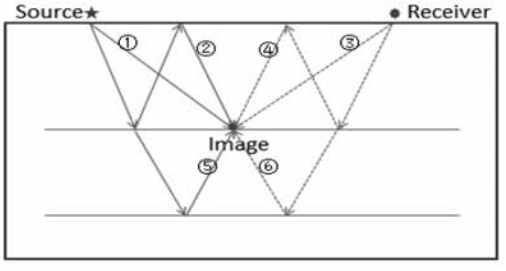

(b)

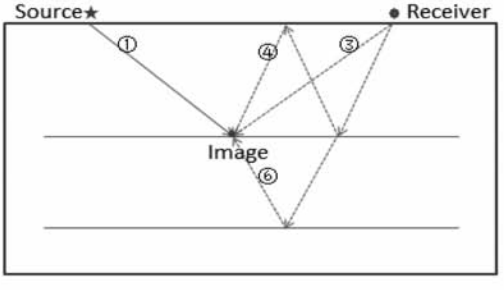

(c)

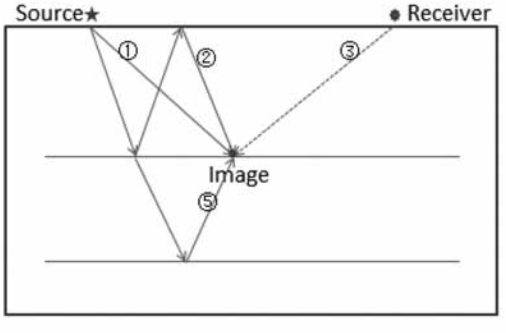

(d)

Fig. 1. Image principles of different migration schemes. (a) One-way wave equation migration; (b) two-way wave-equation migration; (c) one-two-way wave-equation.

SYNTHETIC NUMERICAL EXAMPLES

To verify the imaging ability of the proposed migration, we use two synthetic data sets to compare the performances of different migration schemes. In all numerical simulations, synthetic datasets are computed by using the eight-order finite-difference operator expressed in eq. (4). The four migration methods use the same datasets to implement migration.

Steep dip model

The first model is simple; an inclined layer is set to verify the performance of these migration methods for steep dips. The dip θ is set to 45°, 80° and 90° in the following numerical simulations. The velocity model is depicted in Fig. 2. The horizontal extent of the model is 5,120 ft and its vertical extent is 1,280 ft. The model is meshed to 512 by 128 grids, i.e., spatial grid increments are set to 20 ft in both the vertical and horizontal direction. The velocity of the top layer is 10000 ft/sec, while the increment per layer along the vertical direction is 2000 ft/sec. A total of 128 shots are simulated to implement migration, and all 128 receivers are distributed evenly on the surface. The time increment is set to 0.5 ms, which can ensure computational stability and reduce grid dispersion when the two-way wave-equation is solved in the time-domain. The Ricker wave, with a dominant frequency of 25 Hz, is employed to simulate the amplitude over time of the source. The Perfectly Matched Layer (PML) boundary condition is employed to absorb the energy passing through the boundaries. The synthetic data are preprocessed before migration by muting the direct wave to reduce artifacts (Chang and McMechan, 1986). All computations are implemented using a PC with dominant frequency 3.5 GHz, and codes are

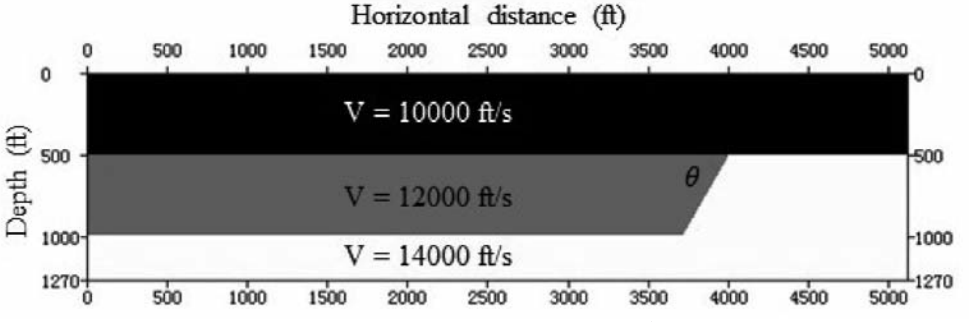

Fig. 2. Dip model.

executed sequentially. It spends 1959 seconds, 3738 seconds, 3779 seconds and 5726 seconds to complete the one-way wave-equation migration, one-two-way wave-equation migration, two-one-way wave-equation migration and two-way wave-equation migration, respectively. There is no obvious difference in storage requirements for the four migration schemes. Thus, it shows that asymmetric wave-equation migration could considerably reduce computation time compared with two-way wave-equation migration, which is consistent with the analysis of complexity.

When the dip is set to 45°, 80° and 90°, the results of the different migration methods are as depicted in Figs. 3-5, respectively. The subfigures (a-d) represent the images produced by using one-way wave-equation migration, two-way wave-equation, one-two-way wave-equation migration, and two-one-way wave-equation migration, respectively. As shown in the figures, one-way wave-equation migration can image the layers clearly with less low-wavenumber artifacts when the dip is equal to 45°. However, as the dip becomes steep, such as 80°, it cannot image the inclined layer effectively. In contrast, two-way wave-equation migration can image all subsurfaces with all dips correctly, but serious low-wavenumber artifacts between layers contaminate the image. Particularly in the strong reflecting subsurface, additional work is needed to filter the image after imaging. The two asymmetric wave-equation migrations can both image the layer with a dip equal to 90°. This indicates that the asymmetric wave-equation migration images without limitation of dips, but the amplitude of the image with steep dips is not very good because it was conducted by RTM. Some low-wavenumber artifacts exist between layers but are not as serious as in two-way wave-equation migration. All subsurfaces can be read directly without the need of any additional post-imaging processing. Compared with the images of two asymmetric wave-equation migration, the one-two-way wave-equation migration can image better than two-one-way wave-equation migration in the numerical simulation. The results indicate that the proposed migration scheme has the ability to image the complex media with less computation and low-wavenumber artifacts.

Hess 2004 Model

We select the Hess 2004 P-wave velocity model as another relatively complicated example to test our imaging condition. The velocity model is depicted in Fig. 6.

We tested and compared the above four migration schemes numerically. In the simulations, we used the same synthetic data but employed different migration schemes. Meanwhile, their performances when using the data with and without direct waves were also compared. Figs. 7-8 show the results based on the four migrations, and subfigures (a-d) are the images produced by using

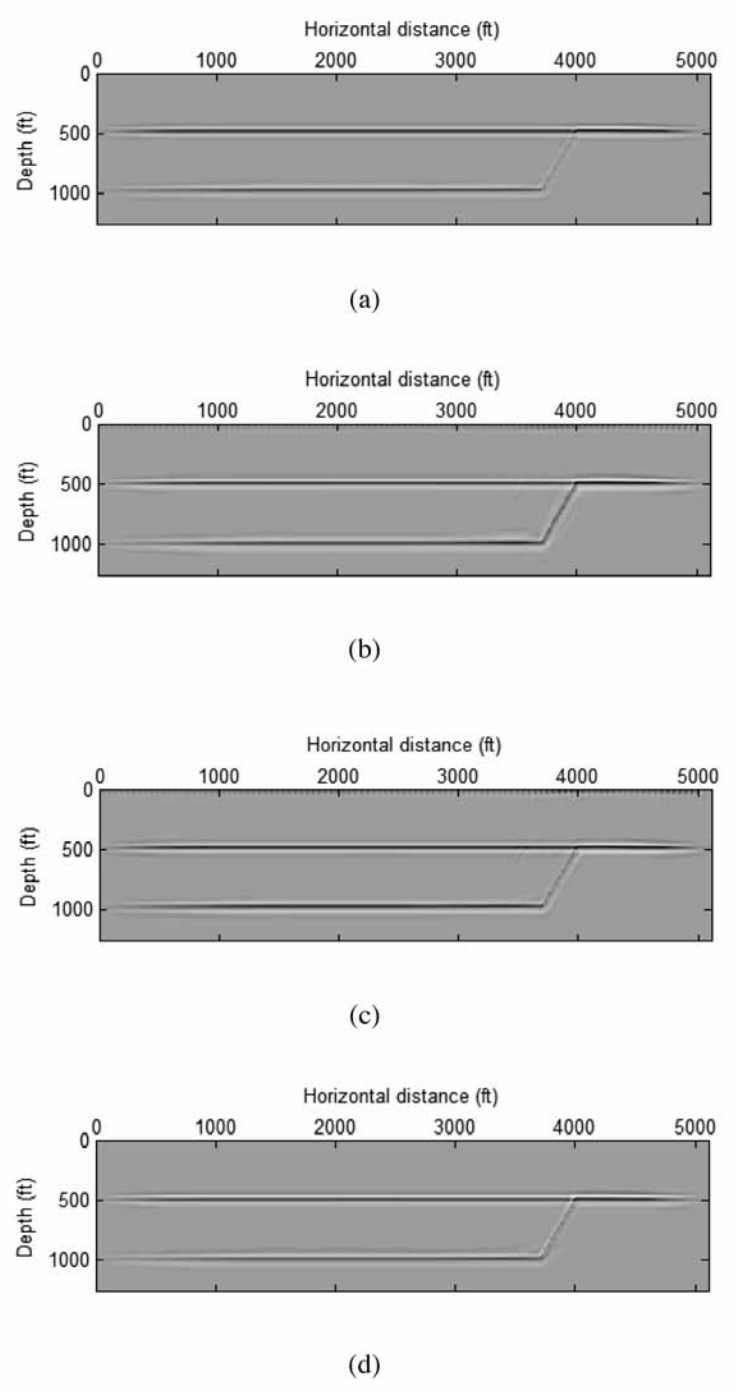

Fig. 3. Images created using different migrations, where the dip is set to 45°. (a) One-way wave-equation migration; (b) two-way wave-equation migration; (c) one-two-way wave equation migration; (d) two-one-way wave-equation migration.

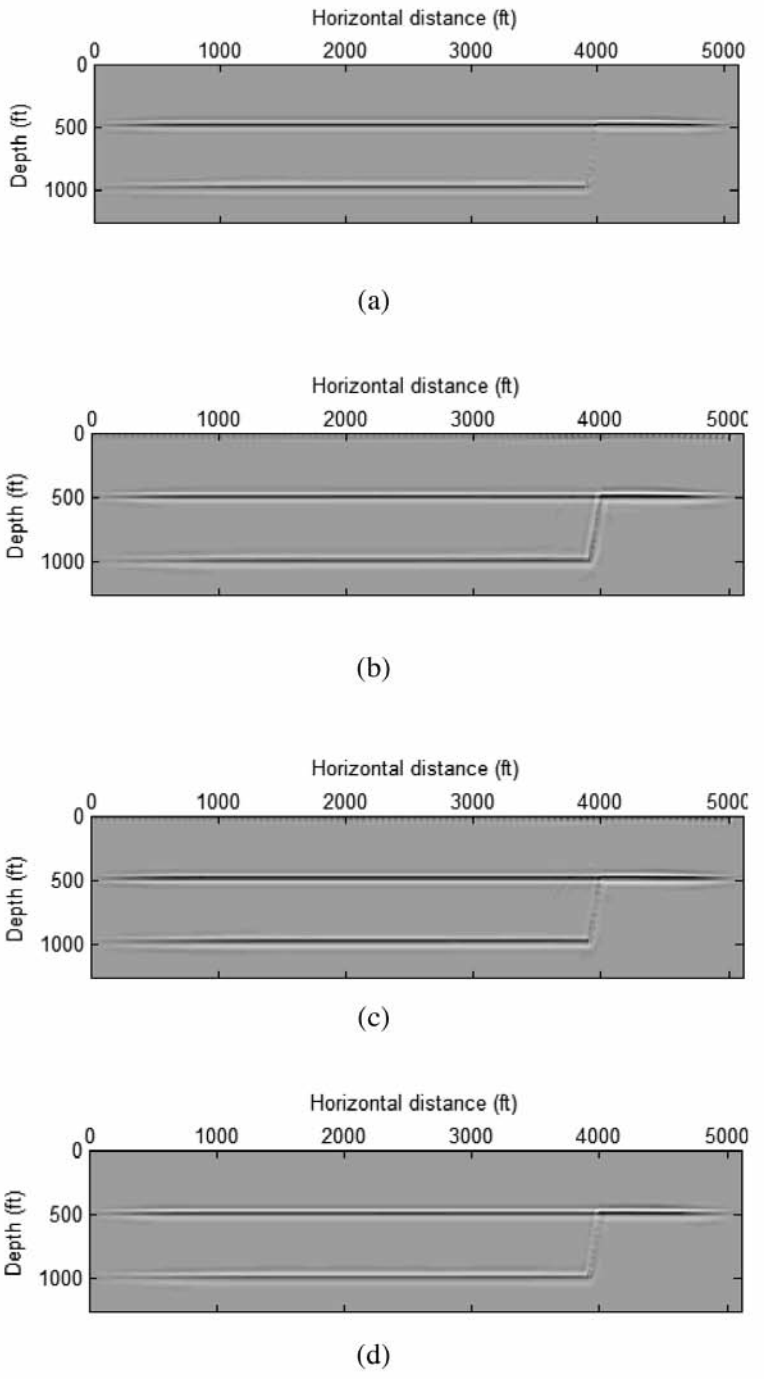

Fig. 4. Images created using different migrations, where the dip is set to 80°. (a) One-way wave-equation migration; (b) two-way wave-equation migration; (c) one-two-way wave equation migration; (d) two-one-way wave-equation migration.

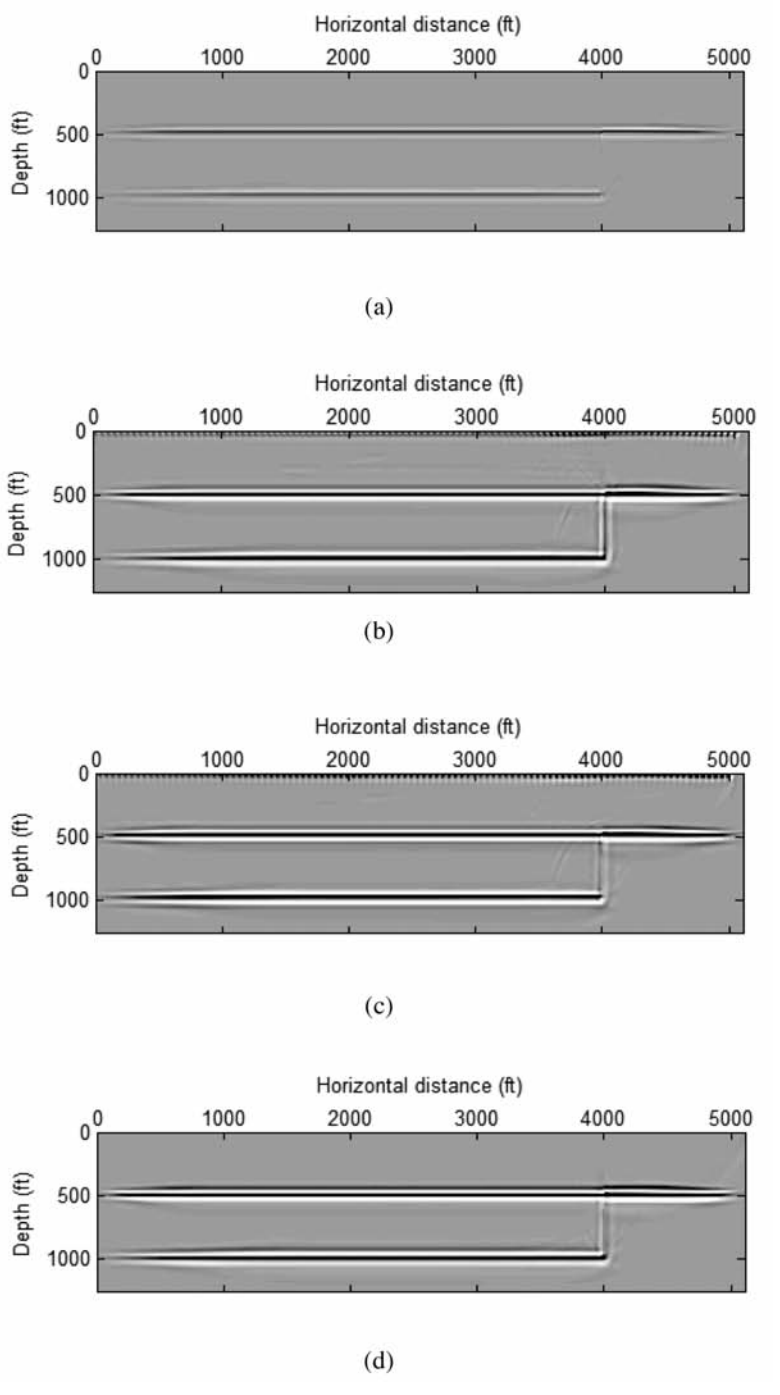

Fig. 5. Images created using different migrations, where the dip is set to 90°. (a) One-way wave-equation migration; (b) two-way wave-equation migration; (c) one-two-way wave equation migration; (d) two-one-way wave-equation migration.

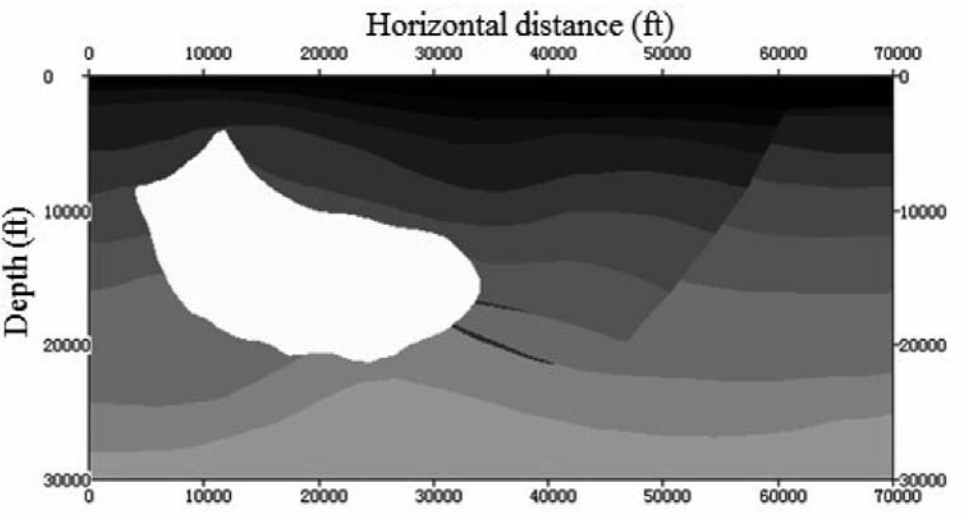

Fig. 6. Hess 2004 P-wave velocity model.

one-way wave-equation migration, two-way wave-equation migration, one-two-way wave-equation migration and two-one-way wave-equation migration, respectively. Fig. 7 is the image created by the filtered seismograph when the direct wave was removed, while Fig. 8 shows the images created by the original seismograph. We can investigate their performance when the interference of direct waves exists. These figures indicate that the one-way wave-equation can image the layers clearly with fewer low-wavenumber artifacts, even for the image created by the original seismograph. However, the left flank of the salt body was not imaged effectively, which is the shortcoming of one-way wave-equation migration. Two-way wave-equation migration works well, even for the surface with steep dips. However, the amount of low-wavenumber artifacts contaminates the images, covering the layers above the salt body wholly if direct waves are not removed. Subfigures (c-d) in Figs. 7-8 show the performances of the proposed asymmetric wave equation migration. The results show that the asymmetric wave-equation migration could image the flanks of the salt body successfully. Moreover, fewer low-wavenumber artifacts appear in the images compared with the images created via two-way wave-equation migration. Even when using the original seismograph without deleting direct waves, only the layers near the surface are contaminated and need additional operations to make them clear.

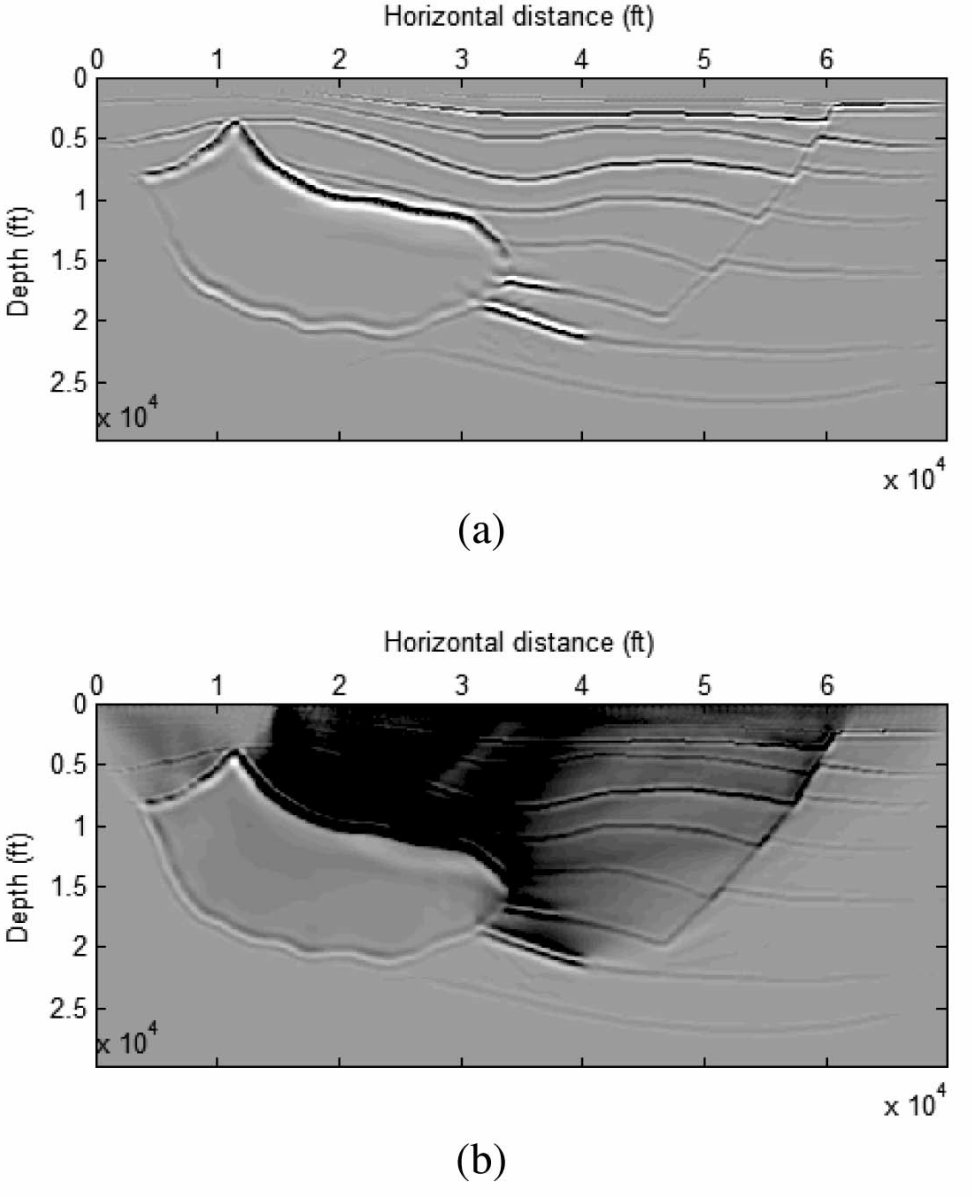

Fig. 7. Images of Hess 2004 model created using different migration schemes, where the direct waves in receivers have been removed in migrations. (a) One-way wave-equation migration; (b) two-way wave-equation migration.

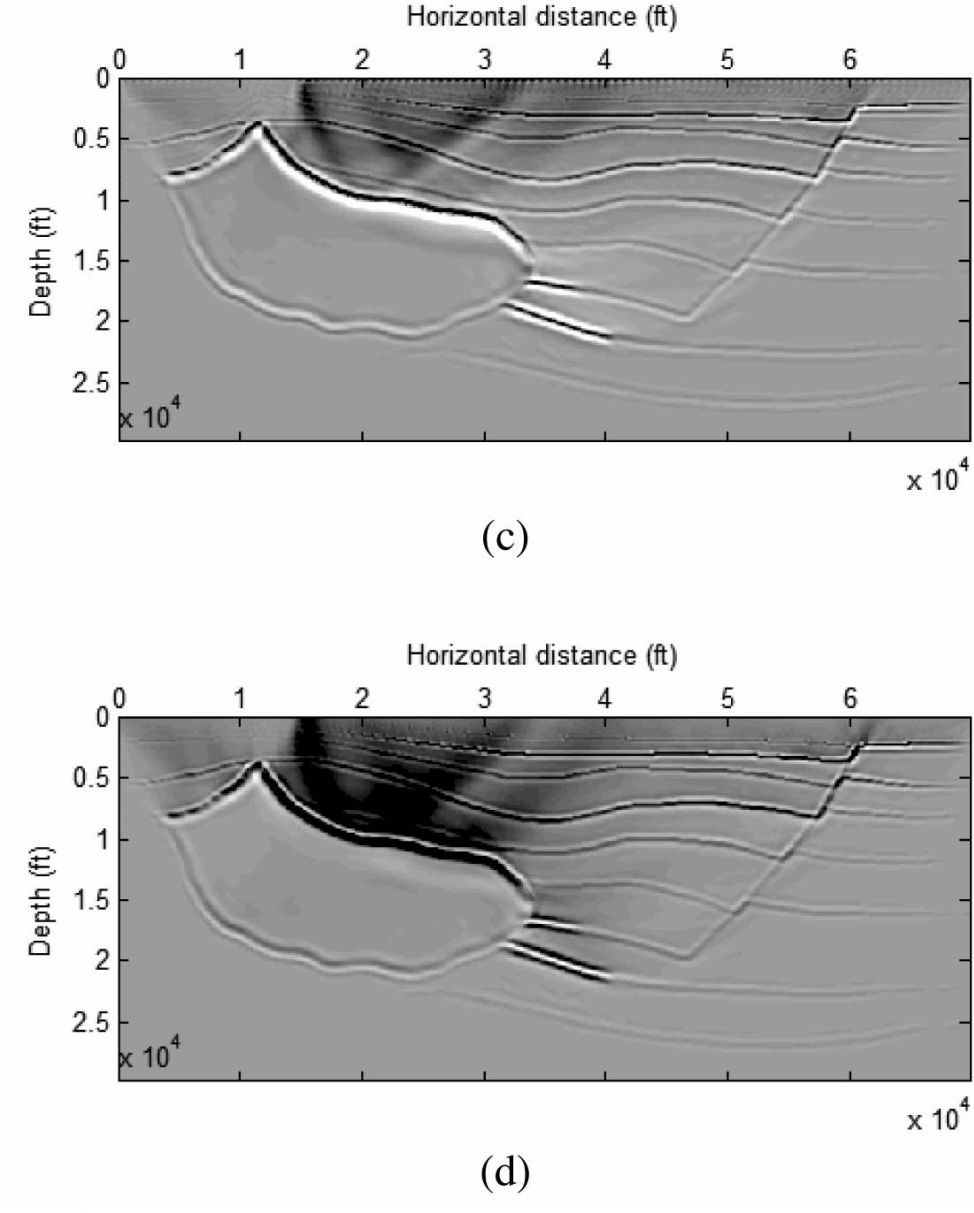

Fig. 7. Images of Hess 2004 model created using different migration schemes, where the direct waves in receivers have been removed in migrations. (c) One-two-way wave-equation migration; (d) two-one-way wave-equation migration.

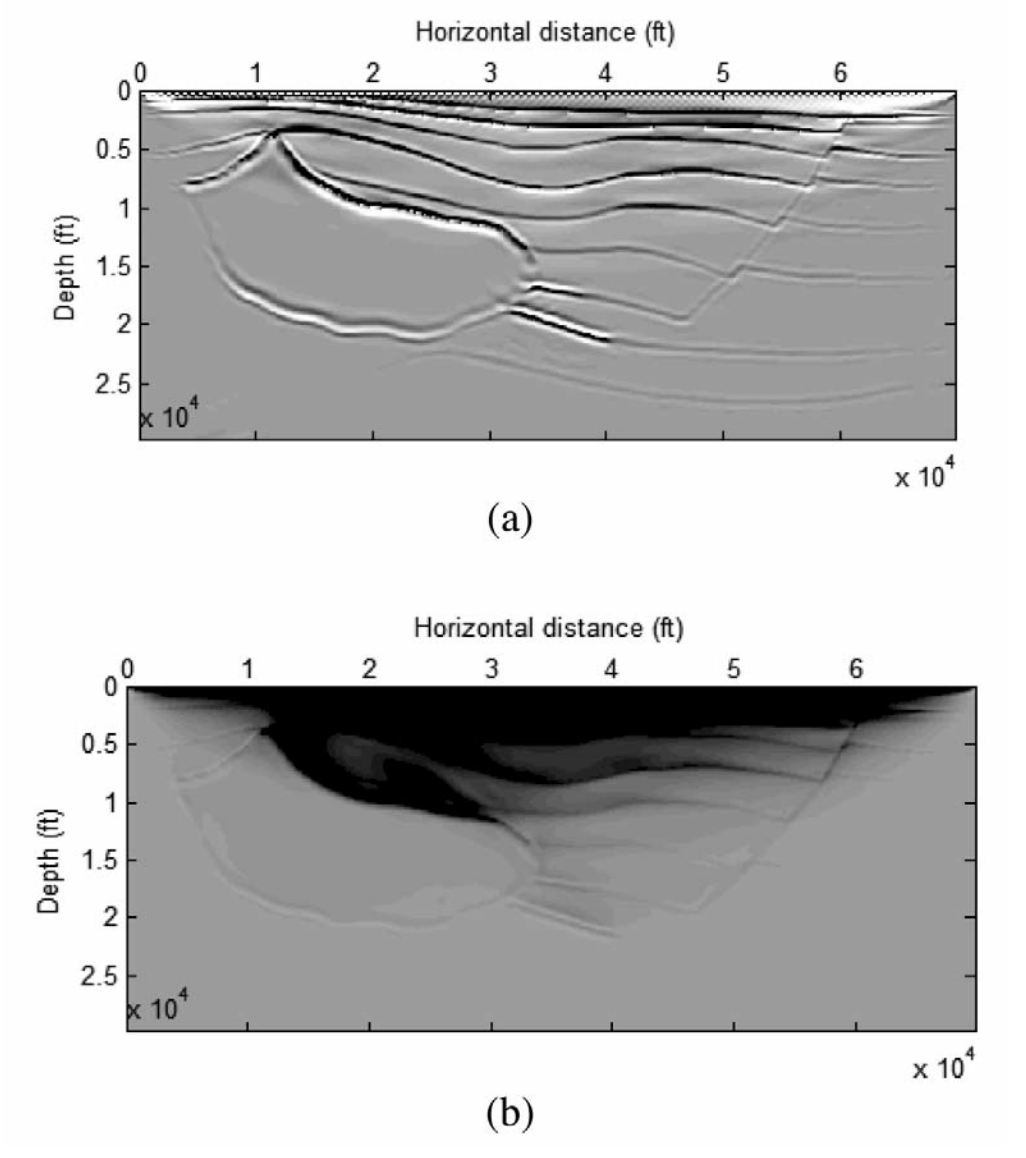

Fig. 8. Images of Hess 2004 model created using different migration schemes, where the direct waves in receivers have not been removed in migrations. (a) One-way wave-equation migration; (b) two-way wave-equation migration.

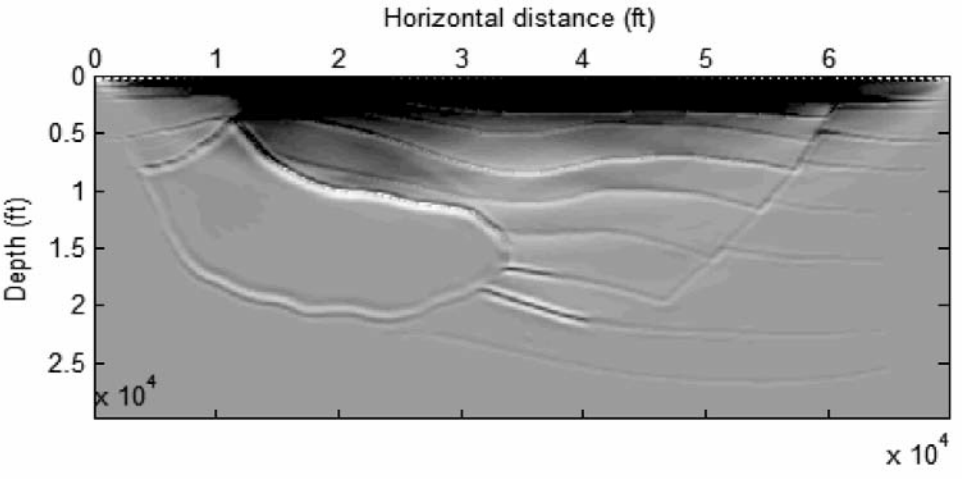

(c)

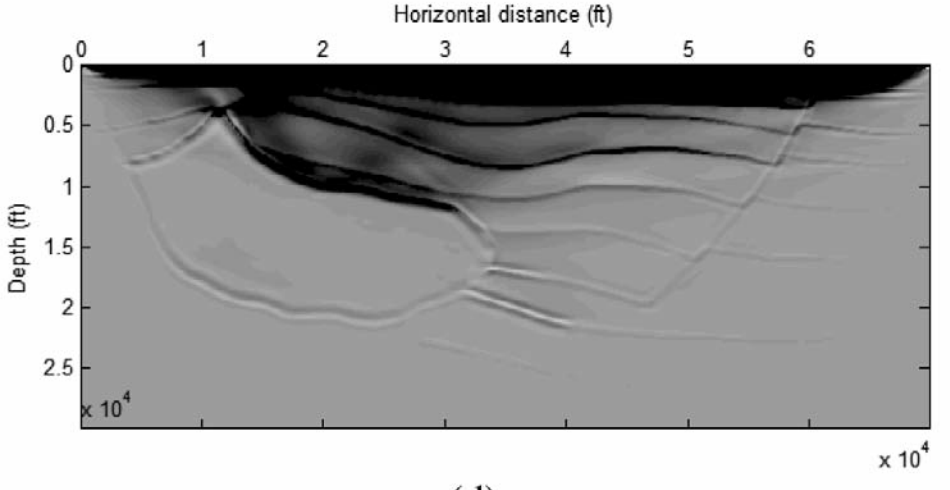

(d)

Fig. 8. Images of Hess 2004 model created using different migration schemes, where the direct waves in receivers have not been removed in migrations. (c) One-two-way wave-equation migration; (d) two-one-way wave-equation migration.

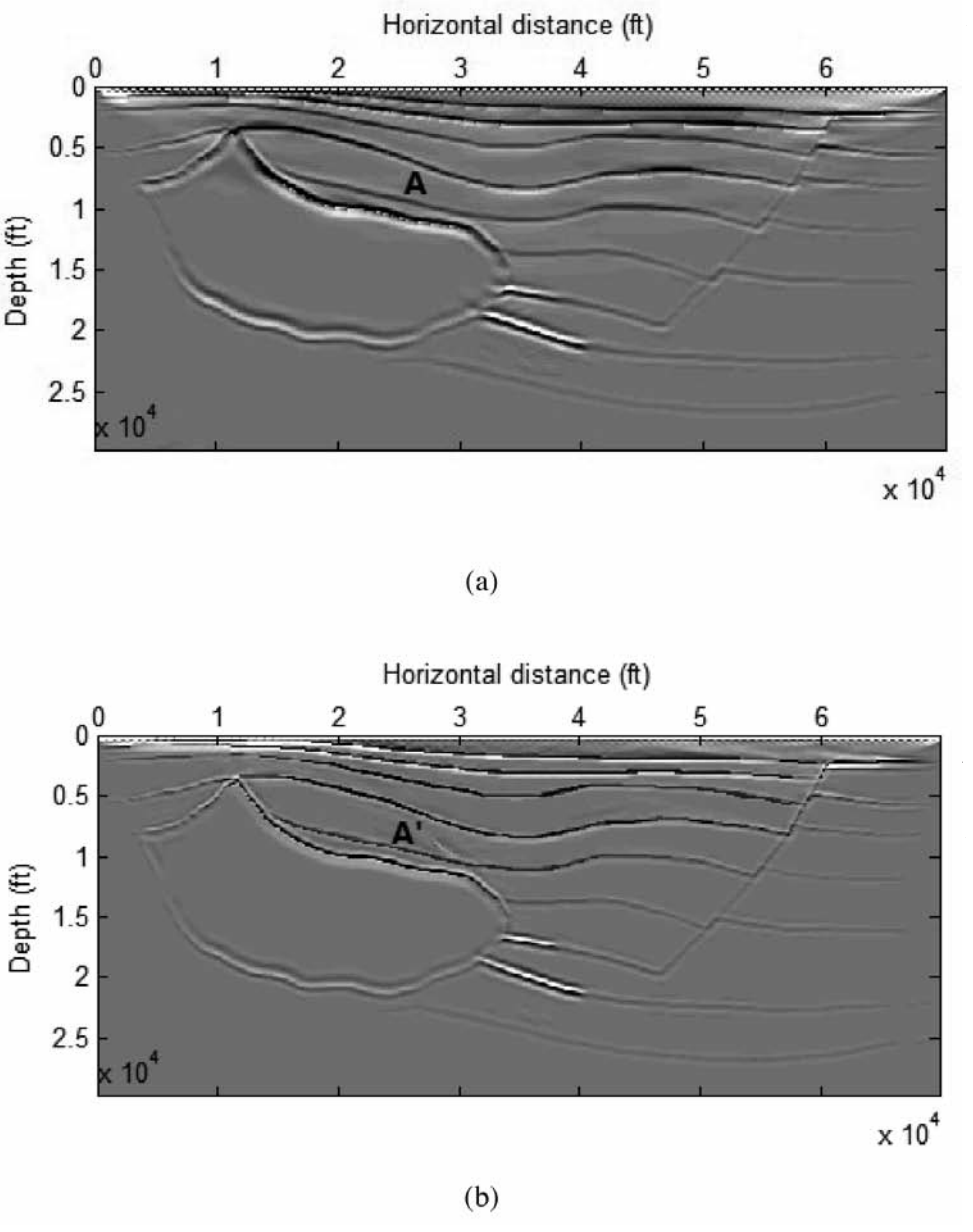

Fig. 9. Images created using one-two-way wave-equation migration and two-way wave equation migration and filtered using the Laplacian operator. (a) One-two-way wave-equation migration; (b) two-way wave-equation migration.

In these cases, we find that one-two-way wave-equation migration works better than two-one-way wave-equation migration. Furthermore, we compared the performances after Laplacian filtering between one-two-way wave equation migration and two-way wave-equation migration. Fig. 9 depicts the results. The results show that the Laplacian operator can remove the majority of low-wavenumber artifacts of low frequency in the two images. Unfortunately, a worse thing appears in the image created using two-way wave-equation migration. An obvious artifact marked as appears above the salt body, which may be the result of incorrect seismic interpretation. However, this artifact does not appear in the image created via one-two-way wave-equation migration. Thus, we conclude that the asymmetric wave-equation migration not only reduces computation time but also reduces artifacts.

CONCLUSIONS

Wave-equation migration is a strong technology for imaging layers. It has become more and more popular recently due to the need for highly accurate seismic interpretation. It can be implemented by using the one-way wave-equation and two-way wave-equation. The former is cheap but cannot image steep dips; the latter is strong but costly and produces an amount of low-wavenumber artifacts. In this investigation, an asymmetric wave-equation migration scheme is developed and provides a midway approach. Thus, if we do not have sufficient computational resources to implement RTM, the asymmetric wave migration scheme is a feasible choice.

Furthermore, two synthetic models are proposed to verify the performance of the asymmetric wave-equation migration compared with other wave-equation migrations. Numerical simulations show that asymmetric wave-equation migration can image without the limitation of dip and produce less low-wavenumber artifacts. Thus, we conclude that it can replace the two-way wave-equation migration when computation resources are limited. This migration approach also offers us a new choice when we fall into the struggle of how to decide between two-way wave-equation migration and one-way wave-equation migration. The numerical results indicate that the asymmetric one-two-way wave-equation migration can image layers effectively. Based on the tests in the investigation, we can conclude regarding the selection of prestack wave-equation migration: if the layers are simple and without steep dips, one-way wave-equation migration is the best choice; if not, and the computational complexity is acceptable, asymmetric wave-equation migration may be the better choice. In the situation where the image of flanks is the key target and the computational complexity is affordable, two-way wave-equation migration is the best.

ACKNOWLEDGMENTS

This work was supported in part by the innovation team fund of Southwest Petroleum University under Grant number 2015CXTD07; we appreciate Dr. Song Guojie for his help.

REFERENCES

Albertin, U., Watts, D., Chang, W., Kapoor, J., Kitchenside, P., Yingst, D. and Stork, C., 2002. Near-saltflank imaging with Kirchhoff and wavefield-extrapolation migration. Expanded Abstr., 72nd Ann. Internat. SEG Mtg., Salt Lake City, 38: 1328-1331.

Bednar, J.B., Stein, J., Yoon, K., Shin, C. and Lines, L., 2003. Two-way-wave equation migration: Overkill or Necessity? Energy Technology Data Exchange.

Baysal, E., Kosloff, D.D. and Sherwood, J.W.C., 1983. Reverse time migration. Geophysics, 48: 1514-1524.

Baysal, E., Kosloff, D.D. and Sherwood, J.W.C., 1984, A two-way nonreflecting wave equation. Geophysics, 49: 132-141.

Biondi, B. and Palacharla, G., 1996. 3-D prestack migration of commonazimuth data. Geophysics, 61: 1822-1832.

Chang, W.F. and McMechan, G.A., 1986. Reverse-time migration of offset vertical seismic profiling data using the excitation-time imaging condition. Geophysics, 51: 67-84.

Chattopadhyay, S. and McMechan, G.A., 2008. Imaging conditions for prestack reverse-time migration. Geophysics, 73(3): 81-89.

Claerbout, J.F., 1971. Toward a unified theory of reflector mapping. Geophysics, 36: 467-481.

Claerbout, J.F., 1985. Imaging the Earth's Interior. Blackwell Science Inc., New York.

Claerbout, J.F., 1998. Multidimensional recursive filters via a helix. Geophysics, 63: 1532-1541.

Collino, F. and Joly, P., 1995. Splitting of operators, alternate directions, and paraxial approximations for the three-dimensional wave equation. SIAM J. Scientif. Comput., 16: 467-481.

Costa, J.C., Silva, F.A., Alcantara, M.R., Schleicher, J. and Novais, A., 2009. Obliquity-correction imaging condition for reverse time migration. Geophysics 3), 74: S57-S66.

Diaz, E. and Sava, P., 2012. Understanding the reverse time migration backscattering: Noise or signal? Expanded Abstr., 82th Ann. Internat. SEG Mtg., Las Vegas: 111-123.

Dablain, M.A., 1986. The application of high-differencing to the scalar wave equation. Geophysics, 51: 54-66.

Fei, T.W., Luo, Y. and Schuster, G.T., 2010. De-blending reverse-time migration. Expanded Abstr., 80th Ann. Internat. SEG Mtg., Denver: 3130-3134.

Feng, L.L., Yang, D.D. and Xie, W., 2015. An efficient symplectic reverse time migration method using a local nearly analytic discrete operator in acoustic transversely isotropic media with a vertical symmetry axis. Geophysics, 80: S103-S112.

Gazdag, J., 1978. Wave equation migration with the phase-shift method. Geophysics, 43: 1342-1351.

Gazdag, J.P. and Sguazzero, P., 1984. Migration of seismic data by phase shift plus interpolation. Geophysics, 49: 124-131.

Guitton, A., Valenciano, A., Sevc, D. and Clearbout, J., 2007. Smoothing imaging condition for shot-profile migration. Geophysics, 72: 149-154.

Huang, L.J., Fehler, M.C. and Wu, R.S., 1999. Extended local Born Fourier migration method. Geophysics, 64: 1524-1534.

Huang, L.J. and Wu, R.S., 1996. Prestack depth migration with acoustic screen propagators. Expanded Abstr., 66th Ann. Internat. SEG Mtg., Denver, 52: 415-418.

Jerome, H., Rousseau, L., Maarten, V. and Hoop, D., 2001. Modeling and imaging with the generalized-screen algorithm in isotropic media. Geophysics, 66: 1551-1568.

Luo, M. and Jin, S., 2008. Hybrid one-way and full-way propagator and migration. Expanded Abstr. 78th Ann. Internat. SEG Mtg., Las Vegas, 73: 881-884.

Liu, F., Zhang, G.Q., Morton, S.A. and Leveille, J.P., 2007. Reverse-time migration using one-way wavefield imaging condition. Expanded Abstr., 77th Ann. Internat. SEG Mtg., San Antonio, 36: 2170-2174.

Liu, F., Zhang, G.Q., Morton, S.A. and Leveille, J.P., 2011. An effective imaging condition for reverse-time migration using wavefield decomposition. Geophysics, 76: 29-39.

McMechan, G.A., 1983. Migration by extrapolation of time-dependent boundary values. Geophys. Prosp., 31: 413-420.

Marfurt, K.J. and Shin, C.S., 1989. The future of iterative modeling in geophysical exploration. In: Supercomputers in Seismic Exploration, Pergamon Press, Inc.: 203-228.

Mulder, W.A. and Plessix, R.E., 2003. One-way and two-way wave-equation migration. Expanded Abstr., 73th Ann. Internat. SEG Mtg., Dallas, 73: 881-884.

Mulder, W.A. and Plessix, R.E., 2004. A Comparison between one-way and two-way wave-equation migration. Geophysics, 69: 1491-1504.

Ren, C.Y., Song, G.J. and Tian, X., 2015. The use of Pointing vector in wavefield decomposition imaging condition for reverse-time migration. J. Appl. Geophys., 112: 14-19.

Ristow D. and Ruhl, T., 1994. Fourier finite-difference migration. Geophysics, 59: 1882-1893.
Sava, P. and Fomel, S., 2006. Time-shift imaging condition in seismic migration. Geophysics, 71: 209-217.

Stoffa, P.L. and Fokkema, J.T. and Freires, M.A., 1990. Split-step Fourier migration. Geophysics, 55: 410-421.

Stolt, R.H., 1978. Migration by fourier transform. Geophysics, 43: 22-48.

Whitmore, N.D., 1983. Iterative depth migration by backward time propagation. Expanded Abstr., 53rd Ann. Internat. SEG Mtg., Las Vegas: 382-385.

Wu, R.S., 1994. Wild-angle elastic wave one-way propagation in heterogeneous media and an elastic wave complex screen method. J. Geophys. Res., 99: 751-766.

Xie, W., Yang, D.H., Liu, F.Q. and Li, J.S., 2014. Reverse-time migration in acoustic VTI media using a high-order stereo operator. Geophysics, 79: WA3-WA11.

Yoon, K. and Marfurt, K.J., 2006. Reverse-time migration using the pointing vector. Explor. Geophys., 37: 102-107.

Zhang, Y. and Sheng, X., Bleistein, N. and Zhang, G., 2007. True-amplitude, angle domain, common-image gathers from one-way wave-equation migrations. Geophysics, 72: 49-58.